Jpn. J. Appl. Phys. Vol. 38 (1999) pp. L 1278–L 1280
Part 2, No. 11A, 1 November 1999

RF Wave Propagation in Bounded Plasma under Divergent and Convergent Magnetic Field Configurations

Seiji TAKECHI[*1] and Shunjiro SHINOHARA[*2]
Interdisciplinary Graduate School of Engineering Sciences, Kyushu University, Kasuga, Fukuoka 816-8580, Japan

(Received February 5, 1999; accepted for publication August 30, 1999)

Radio frequency (RF) wave propagation in a bounded plasma (cylindrical shape with a large diameter of 45 cm) produced by a planar, spiral antenna was investigated under divergent and convergent magnetic field configurations. The measured excited magnetic field amplitude and the phase were examined based on helicon wave characteristics, and were consistent with the computed results using the Transport Analyzing System for tokamaK/Wave analysis by Finite element method (TASK/WF) code. The wave propagation region was broadened (focused) in the radial direction with increasing distance from the antenna under the divergent (convergent) field.

KEYWORDS: RF plasma, wave propagation, spiral antenna, divergent magnetic field, convergent magnetic field, whistler wave, helicon wave, numerical computation

The production of high-density plasma is crucial for plasma processing and confinement devices, and a helicon wave plasma[1–11] and an inductively coupled plasma (ICP)[12–14] are regarded as promising sources. In our previous work,[14,15] in order to produce a high-density plasma with improved uniformity in the radial direction by the ICP scheme with a spiral antenna, we tested various external magnetic field configurations under a relatively low field. We found that the uniformity improved markedly with the cusp field. The results show that there may be a close relationship between the density profile and the radio frequency (RF) wave propagation and absorption regions. Therefore, analysis of the wave characteristics in various field configurations as a control parameter is important for the production of the desired plasma profiles. In addition, the results of the wave analysis would provide us interesting topics related to helicon wave physics with a nonuniform magnetic field, which has been scarcely investigated to date. In previous studies,[16–18] the wave phenomena were examined under the cusp field configuration, while changing the line cusp position as well as the gradient and magnitude of the magnetic field: The excited $m = 0$ mode helicon wave damped strongly near the cusp position, and this wave could propagate beyond this position when the magnetic field strength and/or the gradient of the field near the cusp position was increased. These observations agreed qualitatively with the computed results that the wave propagated along the magnetic field line while avoiding the neutral magnetic field point.

The whistler wave characteristic, which is predicted theoretically, shows that the maximum angle between the direction of the wave group velocity and the magnetic field line is less than 20 degrees in a free space.[19] However, for the helicon wave known as a bounded whistler wave, the relationship between the wave propagation region under limited device geometry and the nonuniform field line was scarcely reported, and must be examined for the development of a plasma production scheme as well as studies of basic wave physics.

In this work, we characterize RF wave propagation under both divergent and convergent magnetic field configurations having a weaker line bending curvature compared to the cusp field. Two-dimensional spatial profiles of the amplitude and the phase of excited magnetic fields in a large-diameter (45 cm) plasma were measured. The results obtained were compared with the results computed using the Transport Analyzing System for tokamaK/Wave analysis by Finite element method (TASK/WF) code developed by A. Fukuyama.[20]

The experimental system is the same as that shown in Fig. 1 of ref. 14. The four-turn, water-cooled, spiral antenna with a diameter of 18 cm was made of copper. The distance between the surface of the antenna and the quartz window, which was 25 cm in diameter and 0.8 cm thick, was 1.7 cm. Here, $z = 0$ cm was defined as the point at the window surface which faces an inner vacuum chamber ∼45 cm in diameter and 170 cm in length. The applied divergent (convergent) magnetic fields were generated by six (five) coils having 48 turns each. Contour plots of the magnetic flux are shown in Fig. 1: (a) divergent, and (b) convergent magnetic field configurations.

The continuous RF input power was ∼300 W with a frequency of 7 MHz and an Ar filling pressure of 8.5 mTorr in our experiments. Ar plasma parameters were measured by the use of movable and rotatable Langmuir (1 mm in diameter with 3 mm length) and magnetic (one turn coil with 7 mm in diameter) probes inserted axially into the plasma (main mea-

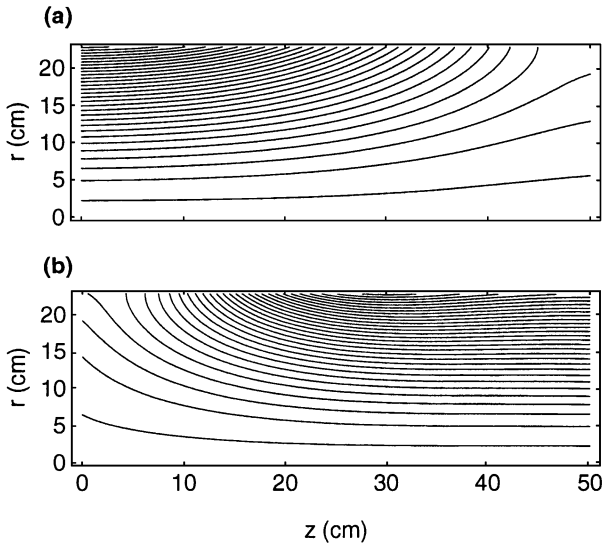

Fig. 1. Contour plots of the magnetic flux (linear scale) with (a) divergent and (b) convergent magnetic field configurations.

[*1]E-mail address: takechi@aees.kyushu-u.ac.jp
[*2]E-mail address: sinohara@aees.kyushu-u.ac.jp

suring region was $z = 4$–50 cm with four radial positions of $r = 0$, 5, 10 and 15 cm). Typical electron temperature T_e was 2–3 eV, and the electron density n_e near the antenna was $\leq 10^{12}$ cm^{-3}.

Figure 2 shows two-dimensional contour plots of (a) the amplitude and (b) the phase of axial components of the excited magnetic field B_z under the divergent field with the coil current $I_c = 20$ A (the magnetic field on the axis at $z = 0$ cm was ~23 G). The intervals between contour lines in Figs. 2(a) and 2(b) were 0.2 in logarithmic scale and $\pi/2$ in linear scale, respectively. It can be seen that the amplitude of B_z was larger on the axis, and the phase at fixed z position changed by $\sim \pi$ radians in the radial direction from the central axis to the wall. Although the radial resolution of 5 cm is poor due to the finite radial measuring positions mentioned above, these characteristics are the same as those of the helicon wave with an azimuthal mode number of $m = 0$ mode. This was also confirmed from the dispersion relation (wave number vs density for a fixed frequency of 7 MHz at $z < 30$ cm) and radial profiles of (azimuthal component) B_θ and B_z at $z = 30$ cm (not shown). It is also shown from Fig. 2(b) that the effective radius of the wave propagation region (related to the position of phase change of $\sim \pi$) increased with increasing z, which is in agreement with the enlarged angle between the magnetic field lines and the z axis (see Fig. 1(a) of divergent magnetic field configuration).

Figure 3 shows two-dimensional contour plots of (a) the amplitude and (b) the phase of B_z under the convergent field with $I_c = 200$ A (the magnetic field on the axis at $z = 0$ cm was ~9 G). Here, the scale and the interval are the same as those in Fig. 2. Although the WKB approximation[19] may not hold, the excitation of the $m = 0$ mode helicon wave is expected for this applied field, considering RF frequency, the dominant antenna current path and the observed radial wave structures in the same way as the above case (divergent magnetic field). Figure 3(a) shows that the region of the excited wave in the radial direction decreased with increasing z. Although there is relatively poor radial resolution as mentioned above, the position of the phase change of $\sim \pi$ in the radial direction in Fig. 3(b) also supports the decrease in the radial wave excited region with increasing z.

Next, the experimentally obtained results were compared with results computed using the TASK/WF code, employing the finite-element method to solve vector and scalar potentials of the wave. This code can analyze wave propagation in an inhomogeneous medium under various external magnetic field configurations. Here, we use a cold-plasma dielectric tensor including collisions with neutrals (the mesh interval was 1 cm in both radial and axial directions). The computation results obtained by the use of four antenna loops with the axial profile of the observed electron density showed the same tendency as the experimental results for the amplitude and phase of the excited B_z under both divergent and convergent fields (data not shown).

In order to check the power deposition profile, the radial profiles of power absorbed by electrons while changing the axial position are computed and shown in Figs. 4(a) and 5(a) under the same conditions as those in Fig. 2 (divergent field) and Fig. 3 (convergent field), respectively. This power absorption is defined as the scalar product of the electron current density J multiplied by the wave electric field E. Figure 4(a) (divergent field) shows that as z increased, the peak position of the power absorption shifted from the central axis to the outer radial position with decreasing absolute absorbed power. Although the effect of change in the radial diffusion with increasing z-position, i.e., decreasing magnetic field strength, must be considered, this result can be considered to partly reflect the experimentally observed spatial profile of the ion saturation current I_{is}: The ratio of I_{is} at $r = 0$ cm to that at $r = 15$ cm was ~3.2 at $z = 4$ cm, while this ratio was ~1.6 at $z = 30$ cm, i.e., a broader profile with z, as shown in Fig. 4(b). Figure 4(a) also shows that the trajectory of the peak power absorption in (r, z) space, which can be used as a measure of the main wave propagation region, did not deviate from the direction of the magnetic field line less than 20 degrees (see also Fig. 1(a)).

From Fig. 5(a) (convergent field), the radial position having the half-value of the peak power absorption decreased as z increased, and did not deviate from the field line direction

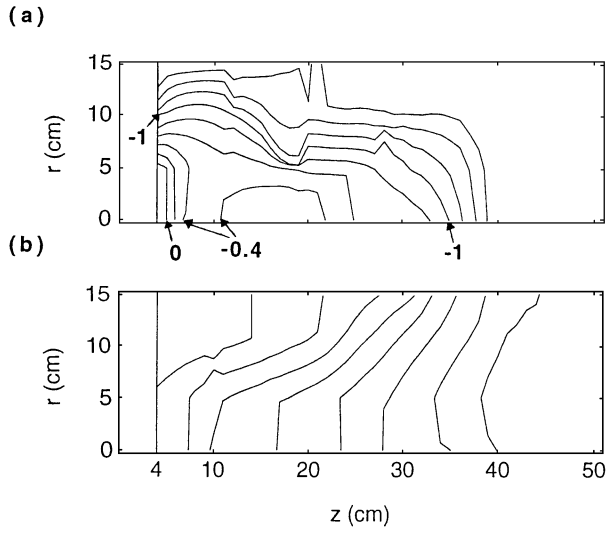

Fig. 2. Contour plots of (a) amplitude (logarithmic scale) and (b) phase (linear scale) of B_z under the divergent field configuration with $I_c = 20$ A.

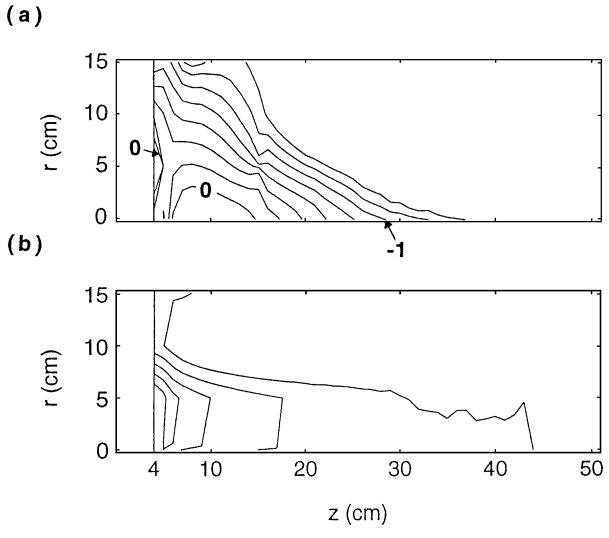

Fig. 3. Contour plots of (a) amplitude (logarithmic scale) and (b) phase (linear scale) of B_z under the convergent field configuration with $I_c = 200$ A.

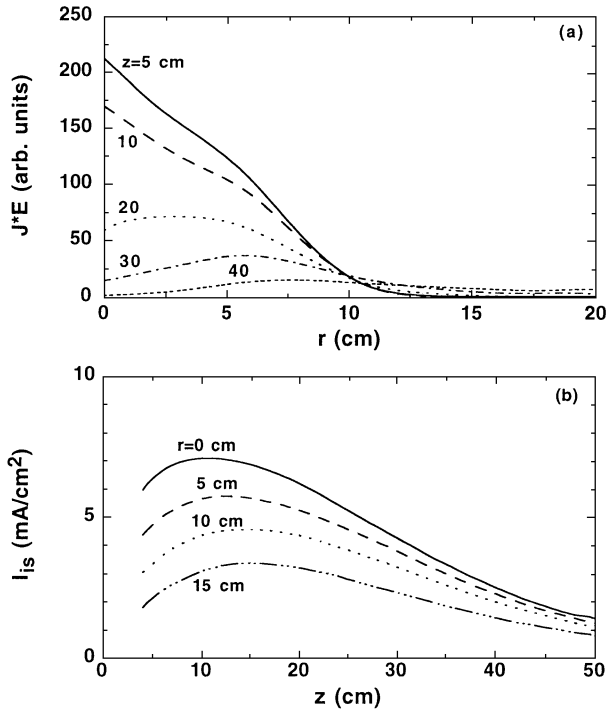

Fig. 4. (a) Radial profiles of computed wave power absorption by electron $J * E$, changing the axial position and (b) experimentally observed spatial profile of ion saturation current I_{is}, under the divergent field configuration with $I_c = 20$ A.

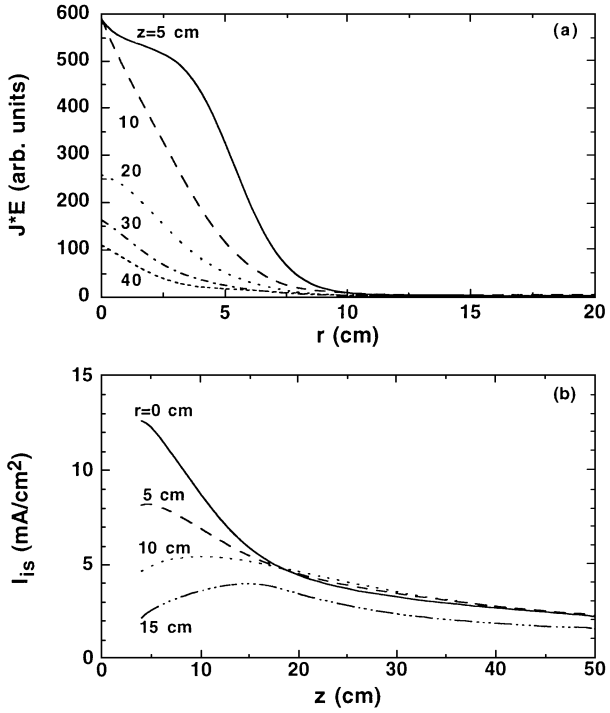

Fig. 5. (a) Radial profiles of computed wave power absorption by electron $J * E$, changing the axial position and (b) experimentally observed spatial profile of ion saturation current I_{is}, under the convergent field configuration with $I_c = 200$ A.

by less than 20 degrees (see also Fig. 1(b)). Nevertheless, the spatial profile of I_{is}, as shown in Fig. 5(b), did not exhibit the peak radial profile expected from the above wave propagation, especially when $z > 10$ cm. The reason for this can be considered as follows. Since the excited helicon wave propagated in a narrower range of r and damped more strongly with z compared with the case of Fig. 4(a), the plasma production region was more limited near the center axis and the antenna, i.e., the sharply peaked density profile (experiment, Fig. 5(b)) and the sharply peaked RF power deposition profile (calculation, Fig. 5(a)). However, near the antenna, the radial diffusion is considered to be large due to the weak field, which causes the rapid flattening of the density profile with $z < 15$ cm; after that, the radial profile could be held almost constant due to the stronger field with z (convergent field, see Fig. 5(b)).

In conclusion, in order to investigate the relationship between the direction of wave propagation and the magnetic field line with not a free boundary but a limited, finite boundary, the characteristics of RF wave propagation under divergent and convergent magnetic field configurations were examined. The measured spatial profiles of amplitude and phase of the excited magnetic field in a large-diameter plasma were consistent with the computation results obtained from the TASK/WF code. The excited $m = 0$ mode helicon wave propagation region became broad (narrow) in the radial direction with z under the divergent (convergent) field, and the wave propagation angle with respect to the magnetic field line direction was less than 20 degrees.

Acknowledgement

We would like to thank Prof. A. Fukuyama for the use of the TASK/WF code, and Prof. Y. Kawai for his continuous encouragement.

1) R. W. Boswell: Plasma Phys. Control. Fusion **26** (1984) 1147.
2) F. F. Chen: Plasma Phys. Control. Fusion **33** (1991) 339.
3) A. Komori, T. Shoji, K. Miyamoto, J. Kawai and Y. Kawai: Phys. Fluids **B3** (1991) 893.
4) T. Shoji, Y. Sakawa, S. Nakazawa, K. Kadota and T. Sato: Plasma Sources Sci. Technol. **2** (1993) 5.
5) Y. Yasaka and Y. Hara: Jpn. J. Appl. Phys. **33** (1994) 5950.
6) M. Light and F. F. Chen: Phys. Plasmas **2** (1995) 1084.
7) S. Shinohara, Y. Miyauchi and Y. Kawai: Plasma Phys. Control. Fusion **37** (1995) 1015.
8) K. Suzuki, K. Nakamura and H. Sugai: Jpn. J. Appl. Phys. **35** (1996) 4044.
9) Y. Sakawa, N. Koshikawa and T. Shoji: Appl. Phys. Lett. **69** (1996) 1695.
10) S. Miyake, Y. Setsuhara, J. Q. Zhang, M. Kamai and B. Kyoh: Surf. Coat. Technol. **97** (1997) 768.
11) S. Shinohara, S. Takechi, N. Kaneda and Y. Kawai: Plasma Phys. Control. Fusion **39** (1997) 1479.
12) J. Hopwood: Plasma Sources Sci. Technol. **1** (1992) 109.
13) J. Hopwood, C. R. Guarnieri, S. J. Whitehair and J. J. Cuomo: J. Vac. Sci. & Technol. **A11** (1993) 147.
14) S. Shinohara, S. Takechi and Y. Kawai: Jpn. J. Appl. Phys. **35** (1996) 4503.
15) S. Takechi, S. Shinohara and Y. Kawai: Jpn. J. Appl. Phys. **36** (1997) 4558.
16) S. Takechi, S. Shinohara and Y. Kawai: Surf. Coat. Technol. **112** (1999) 15.
17) S. Takechi and S. Shinohara: *Proc. 4th Int. Conf. Reactive Plasmas & 16th Symp. Plasma Processing* (Hawaii, 1998) p. 153.
18) S. Takechi, S. Shinohara and A. Fukuyama: Jpn. J. Appl. Phys. **38** (1999) 3716.
19) T. H. Stix: *Waves in Plasmas* (AIP, New York, 1992).
20) A. Fukuyama and Y. Ichida: *Proc. Int. Conf. Plasma Physics* (Nagoya, 1996) Vol. 2, p. 1342.